

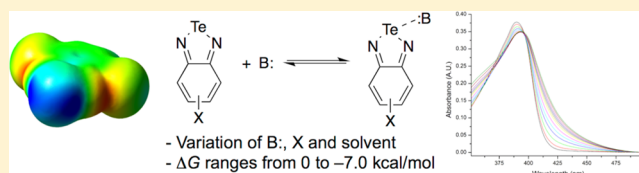
Chalcogen Bonding in Solution: Interactions of Benzotelluradiazoles with Anionic and Uncharged Lewis Bases

Graham E. Garrett, Gregory L. Gibson, Rita N. Straus, Dwight S. Seferos, and Mark S. Taylor*

Department of Chemistry, University of Toronto, Toronto, Ontario M5S 3H6, Canada

S Supporting Information

ABSTRACT: Chalcogen bonding is the noncovalent interaction between an electron-deficient, covalently bonded chalcogen (Te, Se, S) and a Lewis base. Although substantial evidence supports the existence of chalcogen bonding in the solid state, quantitative data regarding the strengths of the interactions in the solution phase are lacking. Herein, determinations of the association constants of benzotelluradiazoles with a variety of Lewis bases (Cl^- , Br^- , I^- , NO_3^- and quinuclidine, in organic solvent) are described. The participation of the benzotelluradiazoles in chalcogen bonding interactions was probed by UV-vis, ^1H and ^{19}F NMR spectroscopy as well as nano-ESI mass spectrometry. Trends in the free energy of chalcogen bonds upon variation of the donor, acceptor and solvent are evident from these data, including a linear free energy relationship between chalcogen bond donor ability and calculated electrostatic potential at the tellurium center. Calculations using the dispersion-corrected B97-D3 functional were found to give good agreement with the experimental free energies of chalcogen bonding.



INTRODUCTION

Noncovalent interactions in which group IV–VII elements act as electrophiles have attracted interest in recent years. Halogen bonding, the most familiar member of this class, was the subject of intensive investigations as early as the 1950s and has seen a resurgence of fundamental studies and new applications over the past decade.¹ It has become increasingly clear that this phenomenon can be generalized to include related interactions, including those of electron-deficient chalcogens² (the group VI elements: S, Se and Te) and pnictogens (group V elements: P, As, Sb).³ In particular, systematic studies of close contacts between nucleophilic sites and electron-deficient, covalently bonded chalcogen atoms in the solid state,⁴ along with computational modeling of $\text{Y}\cdots\text{ER}_2$ complexes (where Y is a nucleophilic moiety, E is a chalcogen and R is an electron-withdrawing group)⁵ provide a compelling argument for the existence of noncovalent “chalcogen bonding” interactions analogous to halogen bonds.

Although the evidence for chalcogen bonding is substantial, and its relevance to crystallization of pharmaceuticals,⁶ solid-state ordering of materials,^{4a} organic reactivity⁷ and folding of biomolecules⁸ has been discussed, data regarding the thermodynamics of the interactions in solution are sparse. Zhao and Gabbai demonstrated that incorporation of a telluronium substituent (R_3Te^+) significantly enhanced the fluoride affinity of a triarylborane receptor, and provided spectroscopic and computational evidence for an attractive $\text{F}^-\cdots\text{TeR}_3$ chalcogen bond.⁹ On the basis of the association constant reported for a control receptor, the contribution of the chalcogen bond to the free energy of fluoride binding in methanol may have been as much as 4 kcal/mol. Data for interactions of uncharged chalcogen-based compounds ER_2

would be of value, especially if comprehensive enough to enable meaningful discussion of trends in donor and acceptor ability.

1,2,5-Chalcogenadiazoles (**1**; Figure 1) attracted our attention as a class of donors that might enable determinations

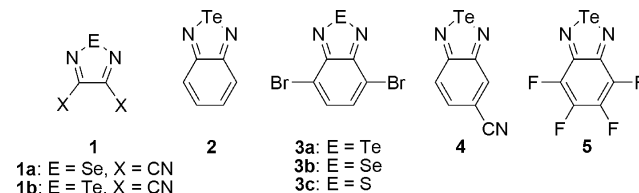


Figure 1. Chalcogenadiazoles and benzochalcogenadiazoles.

of chalcogen bonding association constants in solution. (The generally accepted terminology for these interactions refers to the electron-deficient chalcogen compound as the donor and the Lewis base as the acceptor.) These compounds, particularly the tellurium-bearing congeners, are prone to self-association in the solid state through $\text{N}\cdots\text{chalcogen}$ interactions.¹⁰ Co-crystallization with Lewis basic solvents¹¹ and anions¹² has also been observed. Most relevant to the present study, solution-phase association constants of the highly electron-deficient dicyanotellura- and -selenadiazoles **1a** and **1b** with I^- ($K_a = 6.8 \times 10^5 \text{ M}^{-1}$ in CH_2Cl_2 and $1.5 \times 10^3 \text{ M}^{-1}$ in CH_3CN) and PhS^- ($K_a = 7.4 \times 10^4 \text{ M}^{-1}$ in THF and $3.0 \times 10^3 \text{ M}^{-1}$ in CH_3CN), respectively, were reported during the preparation of this manuscript.¹³ These studies of **1a** and **1b** demonstrated the

Received: December 5, 2014

Published: March 17, 2015

feasibility of determining association constants for this general class of compounds, while raising interesting questions regarding the dependence of the strengths of the interactions on donor, acceptor and solvent identity.

In identifying a specific system for systematic solution-phase studies, we were drawn to benzo-fused chalcogenadiazoles (e.g., **2**), because of their ease of synthesis as well as the prospect of using changes in their UV–vis absorbance or emission spectra to signal chalcogen bonding interactions. In addition, the ability to functionalize the fused six-membered ring provides opportunities to fine-tune chalcogen bond donor ability through substituent effects, or to incorporate this donor group into more complex structures, as exemplified by the synthesis of benzo-chalcogenadiazole-containing conjugated polymers.¹⁴

Here, we describe trends in the solution-phase thermodynamics of chalcogen bonding interactions of benzotelluradiazoles. Binding constants were determined by UV–vis titrations of **2** with anionic and uncharged acceptors in tetrahydrofuran (THF) and acetonitrile. Structure–activity relationships for the chalcogen bond donor were explored by investigating the effects of substitution of the six-membered ring (**3a**, **4**, **5**) and variation of the chalcogen element from Te to Se and S (**3b**, **3c**). Further evidence for the formation of Lewis base–benzotelluradiazole complexes was obtained by nuclear magnetic resonance (NMR) spectroscopy and nanoelectrospray ionization mass spectrometry (nanoESI-MS). Solvent effects on the interaction of **2** with quinuclidine were investigated. Quantum chemical calculations were used to model the complexes, recapitulating trends in chalcogen bond donor and acceptor ability that were evident from the experimental determinations. The results indicate that single-point chalcogen bonding interactions of benzotelluradiazoles can give rise to association constants as high as 10^5 M^{-1} and show considerable variability in strength as a function of the solvent, acceptor, and substitution pattern.

RESULTS AND DISCUSSION

Molecular Electrostatic Potential Calculations for Benzo-chalcogenadiazoles. As a preliminary gauge of the chalcogen bond donor ability of benzo-chalcogenadiazoles, molecular electrostatic potential surfaces were calculated for parent telluradiazole **2** and its substituted derivatives **3a**, **4** and **5**, as well as dibromoselena- and -thiadiazoles **3b** and **3c**, along with the dicyanotelluradiazole **1a** studied by Zibarev and co-workers. The calculations were carried out using Gaussian 09,¹⁵ with the dispersion-corrected B97-D3 functional¹⁶ and the Def2-TZVP basis set.¹⁷ Two “ σ -holes”—regions of electron deficiency centered at the tellurium atom, each situated roughly at the terminus of a Te–N bond—are evident in the electrostatic potential surface of **2** (Figure 2). Viewing the interactions of group IV–VII elements with Lewis bases as electrostatic contacts involving σ -holes provides a rationale for their attractive nature and directionality.¹⁸ In the case of halogen bonding, quantitative correlations between donor ability and the magnitude of $V_{S,\text{max}}$, the electrostatic potential at the point of greatest partial positive charge for the donor atom, have been noted.¹⁹ The calculated $V_{S,\text{max}}$ of 26.3 kcal/mol obtained for benzotelluradiazole **2** suggested that determinations of chalcogen bonding interactions in solution could be feasible: at the same level of theory, a roughly comparable $V_{S,\text{max}}$ of 22.3 kcal/mol was calculated for $\text{C}_6\text{F}_5\text{I}$. The latter is a sufficiently strong halogen bond donor for association

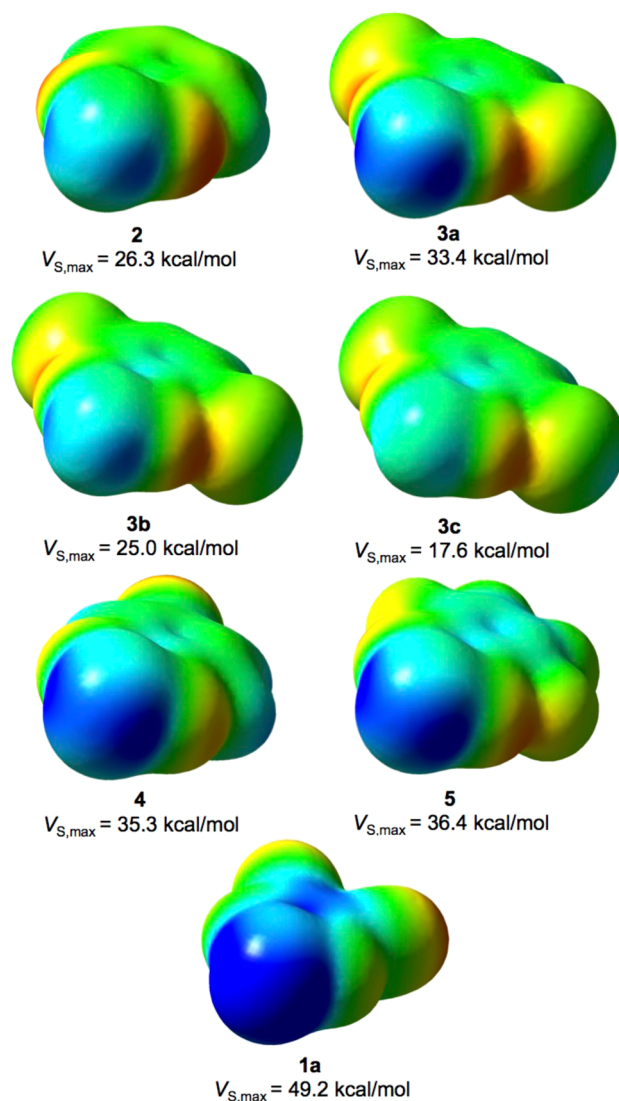


Figure 2. Electrostatic potential surfaces (B97-D3/Def2-TZVP, Gaussian 09) of chalcogenadiazoles **1a**–**5**. Red indicates negative charge density, and blue positive charge density. A common scale was used so that the surfaces can be compared visually.

constants with neutral and anionic Lewis bases to be determined by ^{19}F NMR spectroscopy.^{19a}

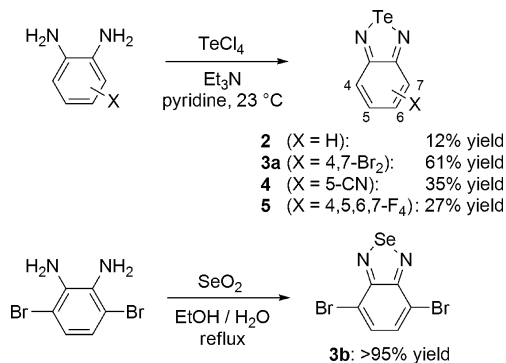
Considerable variation of calculated $V_{S,\text{max}}$ values was observed as a function of the structure and substitution pattern of chalcogenadiazoles **1a**–**5**. Introduction of electron-withdrawing groups to benzo-fused **2** had a significant effect, with dibromo-, cyano- and tetrafluoro-substituted derivatives **3a**, **4** and **5** having values of $V_{S,\text{max}}$ that were 7.1, 9.0, and 10.1 kcal/mol higher than that of **2**, respectively. This result suggested that appreciable tuning of chalcogen bond donor ability would be possible by varying the substituents on the aromatic ring. Consistent with previous computational studies, lower values of $V_{S,\text{max}}$ were obtained for the analogues of **3a** based on the lighter, less polarizable chalcogens (25.0 and 17.6 kcal/mol for **3b** and **3c**, respectively). On the other hand, the $V_{S,\text{max}}$ of dicyanotelluradiazole **1a** (49.2 kcal/mol) is almost twice that of **2**, pointing toward a potent donor ability for this compound.

The trends in donor ability that could be inferred from the electrostatic potential calculations (**1a** > **5** > **4** > **3a** > **2** > **3b** > **3c**) were borne out by the association constants for interactions

of these compounds with Lewis bases in solution (see below). This is not meant to imply, however, that chalcogen bonding interactions of telluradiazoles should be considered as purely electrostatic contacts. Computational studies of halogen bonding suggest that dispersion, polarization and charge-transfer components can contribute appreciably—and to varying extents, depending upon the partners involved—to these interactions.²⁰ Experimental evidence, including solvent effects,^{19a,21} the dependence of the interaction on donor/acceptor structure,^{19a,22} UV–vis absorbance²³ and K-edge X-ray absorption spectral features,²⁴ is consistent with this assertion. Computation also points toward important “nonelectrostatic” contributions to chalcogen bonding interactions, particularly those of tellurium-centered donors.⁵ Nonetheless, relationships between calculated electrostatic potentials and experimental thermodynamics of halogen bonding have been noted for series of structurally related compounds, as described above, and the present study indicates that this also is true of chalcogen bonding interactions.

Synthesis of Benzochalcogenadiazole Donors. Benzochalcogenadiazoles **2**,²⁵ **3a** and **3b**^{11a} were synthesized from the corresponding 1,2-phenylenediamines using previously reported protocols (Scheme 1). These moisture-sensitive compounds were synthesized, purified and stored under inert atmosphere, on a Schlenk line or in a glovebox.

Scheme 1. Synthesis of Benzochalcogenadiazoles



Determinations of Chalcogen Bonding Association Constants in Solution. UV–vis absorbance spectroscopy was employed to determine association constants of **2** with anions (as their tetrabutylammonium salts) in THF. As depicted in Figure 3a, addition of Bu₄N⁺Cl[−] to **2** (15.5 μM in THF) was accompanied by a red-shift of λ_{max} for the benzotelluradiazole chromophore, along with the appearance of a long-wavelength shoulder. The change in absorbance at 416 nm as a function of Bu₄N⁺Cl[−] concentration was fitted to a 1:1 binding isotherm by nonlinear regression analysis to determine the association constant, K_a (Figure 3b). The reported value of K_a (970 ± 10 M^{−1}, Table 1) is the average of the results of five separate titration experiments, and the uncertainty is based on the standard deviation of the multiple determinations.

The stoichiometry of binding was determined to be 1:1 by the method of continuous variation (Job plot analysis, Figure 3c). Although the electrostatic potential calculations revealed two σ-holes for the chalcogen bond donors, no evidence was obtained for the formation of 2:1 complexes with Cl[−] or other anions under the conditions of the titrations. The molar extinction coefficient of **2** in THF was found to be invariant at concentrations up to 100 mM, suggesting that self-association

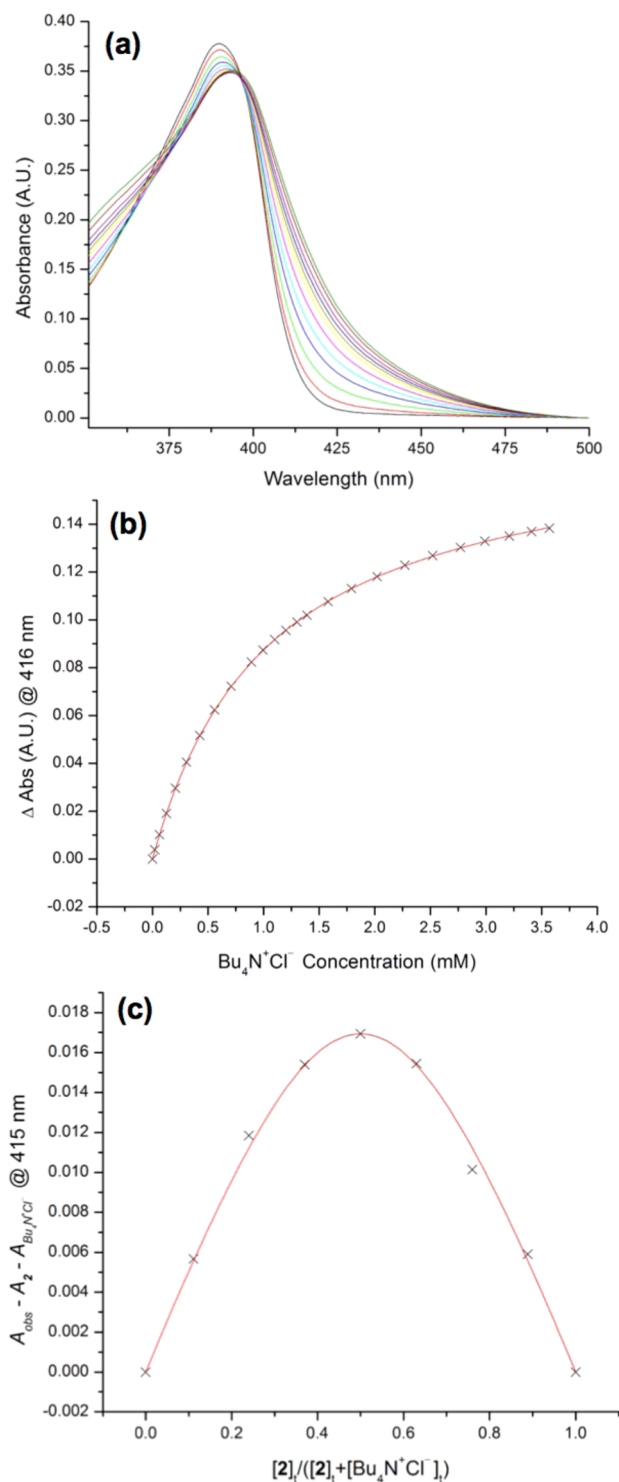


Figure 3. UV–vis titration of **2** (15.5 μM) with Bu₄N⁺Cl[−] in THF. (a) UV–vis absorbance spectral changes upon addition of Bu₄N⁺Cl[−]. (b) Plot of absorbance at 416 nm versus Bu₄N⁺Cl[−] concentration, fit to a 1:1 binding isotherm. (c) Job plot (absorbance change at 415 nm versus mole fraction of **2**, with [2] + [Bu₄N⁺Cl[−]] = 104 mM).

of the donor (through Te⋯N interactions, as has been observed in the solid state) could be discounted under the conditions of the titration.

Addition of Bu₄N⁺Br[−] or Bu₄N⁺NO₃[−] to solutions of **2** in THF was accompanied by red-shifts of the absorbance spectrum similar to that observed with chloride. Association

Table 1. Chalcogen Bonding Association Constants Determined by UV–Vis Absorbance Spectroscopy

donor/solvent	acceptor	K_a (M^{-1}) ^a
2/THF	Cl [−]	970 ± 10
	Br [−]	193 ± 6
	I [−]	<100
	NO ₃ [−]	15 ± 1
	quinuclidine	19.0 ± 0.3
2/CH ₃ CN	Cl [−]	74 ± 1
	Br [−]	30.1 ± 0.4
	I [−]	8.6 ± 0.1
	NO ₃ [−]	<5
	quinuclidine	40 ± 2
3a/THF	Cl [−]	12200 ± 300
	Br [−]	1170 ± 20
	I [−]	– ^b
	NO ₃ [−]	82 ± 4
	quinuclidine	56 ± 5
4/THF	Cl [−]	38000 ± 6000
	Br [−]	2200 ± 200
	I [−]	– ^b
	NO ₃ [−]	80 ± 10 ^b
	quinuclidine	53 ± 4 ^b
5/THF	Cl [−]	130000 ± 20000
	Br [−]	9800 ± 600
	I [−]	– ^b
	NO ₃ [−]	190 ± 10 ^b
	quinuclidine	96 ± 6

^aBinding constants were determined by fitting graphs of UV–vis absorbance change versus acceptor concentration to a 1:1 binding isotherm. Tetrabutylammonium salts of the anionic acceptors were employed. Reported values are the average of three to five independent titration experiments. ^bDonor decomposition occurred over the course of the titration.

constants were found to decrease in the order Cl[−] > Br[−] > NO₃[−] (Table 1). Iodide did not result in sufficiently strong binding for accurate determination of an association constant in THF, and other anions (including H₂PO₄[−], HSO₄[−], AcO[−], TfO[−] and F[−]) caused decomposition of the benzotelluradiazole donor, as judged by UV–vis spectroscopy (see the Supporting Information). At this stage, the products and pathways of these decomposition reactions are not evident. The relative instability of benzotelluradiazoles toward moisture and certain Lewis bases is a limitation that may need to be addressed if their interactions are to be exploited in molecular recognition, catalysis or other applications. The uncharged acceptors tri-*n*-butylphosphine oxide and triphenylphosphine sulfide also resulted in donor decomposition, but an association constant of 19 M^{−1} could be determined for the 2–quinuclidine interaction in THF.

Titrations of **2** in acetonitrile solvent resulted in association constants that were systematically lower than those determined in THF for this set of acceptors. This observation is consistent with the higher polarity and hydrogen bond donor ability ($\alpha = 0.19$ and 0 for CH₃CN and THF, respectively) of acetonitrile relative to THF, and was also noted by the Zibarev group in their investigations of the interactions of **1a** and **1b** with anions.¹³ Due to the relatively high solubility of Bu₄N⁺I[−] in acetonitrile, it was possible to determine the 2–I[−] association constant in this solvent. The trend in the chalcogen bonding association constants of the halides, in both CH₃CN and THF,

parallels that previously observed for halogen bonding, with the most charge-dense anions being the best acceptors. It should be noted that the 2–I[−] association constant in acetonitrile is roughly 2 orders of magnitude lower than that of **1a**–I[−] (1.5×10^3 M^{−1} in CH₃CN).¹³ This result is consistent with the electrostatic potential calculations discussed above, and indicates that the benzotelluradiazoles studied here are significantly weaker donors than dicyanotelluradiazole.

Our preliminary electrostatic potential calculations had suggested that the introduction of electron-withdrawing substituents would enhance the chalcogen bond donor ability of the benzotelluradiazole. Indeed, the association constants of **3a**, **4** and **5** were significantly higher than those of **2** (by more than 2 orders of magnitude, in the case of **5**) across the series of Lewis bases studied here, and increased in the order **3a** < **4** < **5**, consistent with the calculated values of $V_{S,max}$. A linear free energy relationship between log(K_a) for Cl[−] binding and calculated $V_{S,max}$ was observed, with a correlation coefficient $r^2 = 0.98$ (see the Supporting Information). The 5–Cl[−] association constant in THF (130 000 M^{−1}) is roughly equal to that obtained for Cl[−] binding by an electron-deficient *N,N*-diaryurea in the same solvent.²⁶ These results indicate that chalcogen bonding interactions of benzotelluradiazoles can possess significant strength in organic solvent, and can be tuned in a rational way by the introduction of substituents. We note that compound **4**, which lacks substituents at the 4- and 7-positions, appeared to be particularly prone to decomposition in the presence of moisture or Lewis bases.

To rule out other conceivable modes of interaction with benzotelluradiazole **3a** (for example, halogen bonding interactions with the bromo groups, or anion–arene interactions with the electron-deficient π system), titrations of its lighter chalcogen analogues with Bu₄N⁺Cl[−] were conducted in THF. Benzoseladiazole **3b** displayed minimal changes in its absorbance spectrum, and only at high Cl[−] concentrations, suggesting an association constant too low for accurate determination, while the corresponding benzothiadiazole **3c** displayed no spectral changes upon addition of Bu₄N⁺Cl[−]. These observations suggest that the association constants assembled in Table 1 are indeed the result of chalcogen bonding interactions involving the electron-deficient tellurium atom.

Solvent Effects on the Benzotelluradiazole–Quinuclidine Chalcogen Bond. Solvent effects on halogen bonding interactions have been investigated in some detail,^{19a,21,22a} and distinctions between halogen bonding and hydrogen bonding in this regard have been noted. A striking case is the I₂–tetramethylthiourea interaction, which displays similar association constants in *n*-octane and methanol. This result was interpreted as reflecting a dominant “nonelectrostatic” contribution to the halogen bonding interaction that renders it relatively insensitive to changes in solvent polarity and less susceptible to competition from solvent-derived, “harder” acidic or basic sites. It was thus of interest to us to determine whether the soft, polarizable tellurium-centered donors studied here would also differ from typical hydrogen bond donors in terms of solvent effects. Since solvent effects on anion binding are often dominated by anion solvation/desolvation thermodynamics, we elected to use the neutral acceptor quinuclidine for this purpose (Table 2).

The 2–quinuclidine association constant showed only modest variation across the five solvents examined. However, the solvent dependence of this chalcogen bonding interaction

Table 2. Solvent Effects on the Association Constant for the Interaction of 2 with Quinuclidine

solvent	K_a^a
toluene	82 ± 2
CH ₂ Cl ₂	55 ± 3
CH ₃ CN	40 ± 2
acetone	27 ± 1
THF	19 ± 0.3

^aBinding constants were determined by fitting graphs of UV–vis absorbance change versus acceptor concentration to a 1:1 binding isotherm. Reported values are the average of three to five independent titration experiments.

apparently differs from that of the perfluoro-*tert*-butanol–tributylphosphine oxide hydrogen bonding interaction: the free energies of these two interactions showed a poor correlation ($r^2 = 0.71$) for this set of solvents. (The correlation with the free energies of the “solvent-resistant” I₂–tetramethylthiourea interaction was also poor, consistent with the less polarizable nature of the 2–quinuclidine pair relative to this soft XB pair.) Data in a wider range of media are needed to make general conclusions regarding solvent effects on chalcogen bonding, and to uncover the differences between it and other noncovalent interactions in this regard.

Studies of Chalcogen Bonding Interactions of Benzotelluradiazoles by NMR Spectroscopy and ESI-MS. To validate the association constants determined by UV–vis spectroscopy, the interaction of 2 and Bu₄N⁺Cl[−] was studied by ¹H NMR spectroscopy in THF-*d*₈. Upon addition of Bu₄N⁺Cl[−], upfield shifts of the two resonances corresponding to the hydrogens bonded to the benzo-fused ring were observed, consistent with 2 acting as an acceptor of electron density (Figure 4). The magnitude of the change in chemical shift was greater for the hydrogens at positions 5 and 6 (see Scheme 1 for the numbering of positions). The graph of chemical shift change versus concentration of Bu₄N⁺Cl[−] could be fit to a 1:1 binding isotherm, yielding an association constant of 670 ± 30 M^{−1}, which is in reasonably good agreement with the value of 970 ± 10 M^{−1} determined by UV–vis spectroscopy. It should be noted that because the THF-*d*₈ used in this experiment was not dried rigorously, decomposition of 2 to *ortho*-phenylenediamine was evident over the course of the NMR titration. For this reason, and because the NMR titration was not carried out in triplicate, the K_a value determined by UV–vis spectroscopy is likely to be more reliable.

In the case of tetrafluorinated 5, Cl[−] binding in THF-*d*₈ was accompanied by changes in the ¹⁹F NMR spectrum. A significant upfield shift of the signal corresponding to the fluorine groups at the 5- and 6-positions was observed in the presence of Bu₄N⁺Cl[−] (see the Supporting Information). This change is consistent with 5 acting as an acceptor of electron density in a noncovalent interaction, and parallels that observed for halogen bonding interactions of iodoperfluoroarene derivatives.

The interactions between the benzotelluradiazoles and Cl[−] were further studied by negative ion mode nanoESI mass spectrometry. A solution of 3a (257 μM) and Bu₄N⁺Cl[−] (14.3 μM) in THF was introduced into the mass spectrometer, and the 3a–Cl[−] complex isolated with a quadrupole mass filter (50 *m/z* isolation window), thus removing signals corresponding to Bu₄N⁺Cl[−] clusters that otherwise dominated the mass

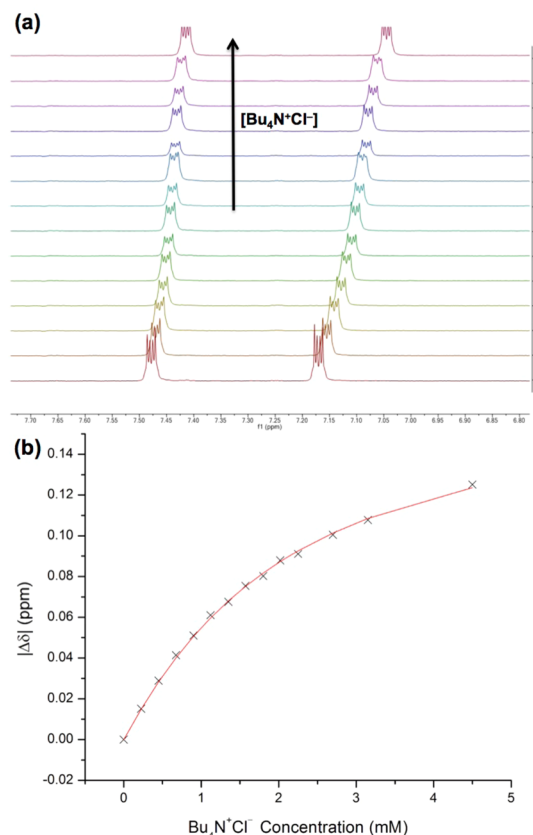


Figure 4. ¹H NMR titration of 2 (0.96 mM) with Bu₄N⁺Cl[−] in THF-*d*₈. (a) ¹H NMR spectral changes upon addition of Bu₄N⁺Cl[−]. (b) Plot of the change in chemical shift |Δδ| versus Bu₄N⁺Cl[−] concentration, fit to a 1:1 binding isotherm.

spectrum. The ions were then transferred into an ion cyclotron resonance cell for analysis. A signal corresponding to the anion–molecule complex was evident at *m/z* = 426.738 (the expected *m/z* for C₆H₂Br₂ClN₂Te[−] is 426.732), displaying the complex isotope distribution that would be expected for such a species (due to the presence of five isotopes of Te with abundance higher than 4%, along with the two isotopes of Cl and Br: see the Supporting Information). A similar experiment was attempted using unsubstituted benzotelluradiazole 2. Perhaps due to the lower affinity of 2 for Cl[−], the chalcogen-bonded complex was not observed by ESI-MS in this case.

Computational Modeling of Benzochalcogenadiazole–Lewis Base Interactions. To assess whether the trends that emerged from our experimental study could be modeled by computation, we carried out DFT calculations on the complexes of 2, 3a, 4 and 5 with Cl[−], Br[−], I[−], NO₃[−] and quinuclidine, as well as other Lewis bases that could not be studied experimentally. Two DFT functionals were investigated: the dispersion-corrected B97-D3¹⁶ method (see above) and M06-2X, which is useful for modeling the thermodynamics of diverse noncovalent interactions.²⁷ The Def2-TZVP basis set was employed for these calculations. Both B97-D3¹³ and M06-2X²⁸ have been employed in previously reported computational studies of chalcogen bonding interactions. The structures obtained after geometry optimization were found to be minima on the potential energy surface, lacking imaginary frequencies, with the exception of a subset of the complexes of quinuclidine and NO₃[−], which showed low imaginary frequencies corre-

sponding to twisting of the quinuclidine or out-of-plane bending of the nitro group (see the Supporting Information).

The calculated (B97-D3) gas-phase geometries of the 2-Cl⁻, 2-Br⁻, 2-I⁻ and 5-Cl⁻ complexes are shown in Figure 5, with

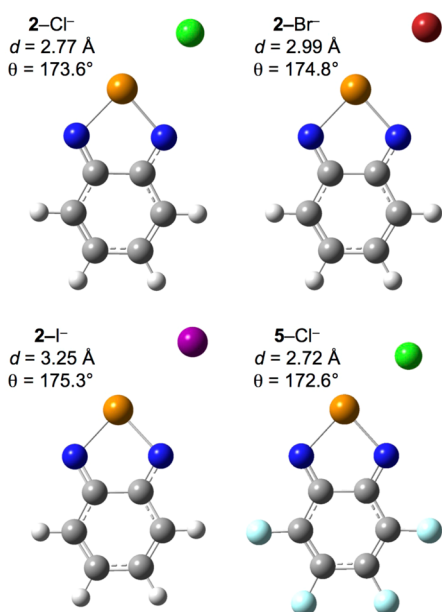


Figure 5. Calculated geometries (B97-D3/Def2-TZVP, gas phase) of the 2-Cl⁻, 2-Br⁻, 2-I⁻ and 5-Cl⁻ complexes. The Te...X⁻ chalcogen bond distance *d* and N-Te...X⁻ angle θ are listed for each structure.

the Te...X⁻ distances *d* and N-Te...X⁻ angles θ noted beside each structure. In all cases, the Te...X⁻ distances are significantly shorter than the sum of the van der Waals radii (Σ_{vdW}) of the two atoms, ranging from 71.3% of Σ_{vdW} for 5-Cl⁻ to 80.4% for 2-I⁻. The Te...X⁻ distances (both in terms of absolute value and as a fraction of Σ_{vdW}) increase in the order Cl⁻ < Br⁻ < I⁻. A comparison of the geometries of 2-Cl⁻ and 5-Cl⁻ reveals a lower calculated chalcogen bond length for the stronger donor ($d = 2.77$ and 2.72 \AA , respectively). The calculated chalcogen bond angles θ range from 173° to 175° , displaying the preference for linearity that was also evident in previous computational and crystallographic investigations. The anions are slightly but systematically displaced toward the proximal nitrogen atom of the benzotelluradiazole, a tendency that is also apparent in crystal structures of telluradiazole-Lewis base adducts.¹¹⁻¹³ A closer inspection of the molecular electrostatic potential surface of 2 suggests a rationale for this effect: whereas the σ -hole of the halogen bond donor C₆F₅I is centered at precisely 180° from C-I, that of 2 is "pulled" slightly toward the proximal nitrogen atom (Figure 6).^{18c}

The gas-phase geometries of the 2-H₂PO₄⁻ and 2-HSO₄⁻ complexes displayed an interesting structural feature: in addition to the expected O...Te chalcogen bonding interaction, a hydrogen bonding interaction between the acidic OH group of these anions and the telluradiazole nitrogen was evident in these structures (see the Supporting Information). Whether the rapid decomposition of 2 in the presence of H₂PO₄⁻ and HSO₄⁻ is a consequence of this complexation mode is unclear.

The calculated free energies of chalcogen bonding interactions of 2, 3a, 4 and 5 are listed in Table 3. Both the PCM and CPCM methods were evaluated to account for solvent effects, with the former providing better quantitative

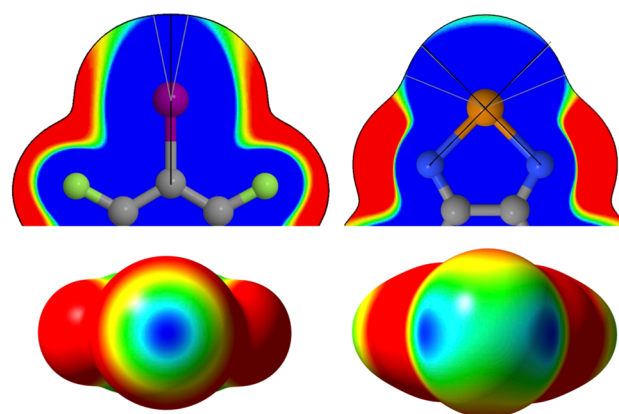


Figure 6. Electrostatic potential maps of C₆F₅I and 2. The electrostatic potentials were calculated in the plane of the ring up to an electron density of 0.001 electrons/bohr³. The color scale was set to range from 0.0 kcal/mol (red) to the $V_{S,max}$ value at 0.001 electrons/bohr³ (blue). Black lines show the extensions of the C-I and N-Te bonds, while gray lines show the σ hole sizes and positions.

Table 3. Experimental and Calculated Free Energies of Chalcogen Bonding Interactions in THF Solvent

complex	$\Delta G_{\text{experiment}}^a$ (kcal/mol)	$\Delta G_{\text{B97-D3}}^b$ (kcal/mol)	$\Delta G_{\text{M06-2X}}^b$ (kcal/mol)
5-Cl ⁻	-7.0	-7.5	-6.2
4-Cl ⁻	-6.2	-6.7	-5.1
3a-Cl ⁻	-5.6	-6.5	-5.6
5-Br ⁻	-5.4	-4.6	-4.3
4-Br ⁻	-4.6	-3.7	-2.5
3a-Br ⁻	-4.2	-4.5	-1.6
2-Cl ⁻	-4.1	-3.5	-2.4
2-Br ⁻	-3.1	-1.2	-0.4
5-NO ₃ ⁻	-3.1	-2.7	ND
5-quinuclidine	-2.7	-3.6	-2.5
3a-NO ₃ ⁻	-2.6	-0.2	+0.4
4-NO ₃ ⁻	-2.6	-2.1	-0.3
3a-quinuclidine	-2.4	-2.2	-0.7
4-quinuclidine	-2.4	-2.7	-1.1
2-quinuclidine	-1.7	-0.9	+0.2
2-NO ₃ ⁻	-1.6	-0.7	+1.3

^aFree energies of interaction were calculated from the association constants determined by UV-vis spectroscopy in THF. Anions were added as the Bu₄N⁺ salts. ^bCalculations employed the Def2-TZVP basis set and the PCM solvent model for THF.

agreement with the experimental data. As shown in Figure 7, the B97-D3 method captures the major trends that were observed experimentally in THF, and appears to slightly outperform the M06-2X functional in this regard.²⁹ Previous studies have highlighted the importance of accounting for dispersion contributions when modeling chalcogen bonding interactions.^{5d}

Time-dependent DFT (TD-DFT) calculations were used to simulate the gas-phase UV-vis absorbance spectra of 2 and 2-Cl⁻. The double-hybrid functional B2PLYP and Def2-TZVP basis set were employed for these calculations,¹³ which were conducted using ORCA 3.0.2. The calculated wavelength of maximum absorbance of the complex 2-Cl⁻ was red-shifted relative to that of the isolated donor 2 (see the Supporting Information), a result that is consistent with the experimental observations from the UV-vis titration studies discussed above.

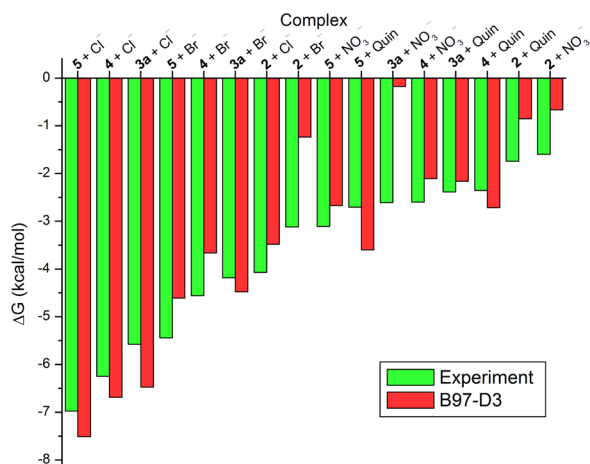


Figure 7. Free energies of chalcogen bonding interactions of **2–5** with Cl^- , Br^- , NO_3^- and quinuclidine (quin). Experimental data in THF solvent (Bu_4N^+ salts for anionic acceptors), along with free energies calculated using the B97-D3 functional (Def2-TZVP basis set, PCM model for THF) are depicted.

CONCLUSION

The addition of Lewis bases to benzotelluradiazoles results in changes in UV–vis and ^1H NMR spectra that can be employed to determine association constants in organic solvents. The interactions of benzotelluradiazoles with anions are of appreciable strength (free energies of interaction as high as 7.0 kcal/mol), and are most favorable for charge-dense Lewis bases such as Cl^- . The significantly enhanced donor ability of the electron-deficient derivatives **3a**, **4** and **5** demonstrates that considerable tuning is possible through variation of the aromatic substituents. Linear free energy relationships between chalcogen bond donor ability and calculated electrostatic potential at Te are evident from these data. The association constant of **2** with quinuclidine shows rather modest variation across a range of solvents (toluene, dichloromethane, acetone, acetonitrile and THF), and in a way that appears to differ from that of hydrogen bonding interactions. Calculations (particularly the dispersion-corrected B97-D3 functional) provide good levels of quantitative agreement with the thermodynamic data in THF solvent. These observations indicate that further explorations of chalcogen bonding in molecular recognition and catalysis are warranted, and that benzochalcogenadiazoles may be a useful starting point for such efforts.

ASSOCIATED CONTENT

Supporting Information

Experimental procedures, characterization data, titration curves and Job plots, methods of data analysis and computational details. This material is available free of charge via the Internet at <http://pubs.acs.org>.

AUTHOR INFORMATION

Corresponding Author

*mtaylor@chem.utoronto.ca

Notes

The authors declare no competing financial interest.

ACKNOWLEDGMENTS

NSERC (Discovery Grants and Canada Research Chair Programs, Graduate Scholarship to G.E.G.), the Province of

Ontario (Ontario Research Fund, Trillium Scholarship to R.N.S.; Queen Elizabeth II Graduate Scholarship in Science and Technology to G.L.G.), and the Canada Foundation for Innovation are gratefully acknowledged for supporting this research. D.S.S. and M.S.T. are Research Fellows of the A. P. Sloan Foundation. D.S.S. is grateful to DuPont for a Young Professor Grant. Calculations were carried out using the High Performance Computing Virtual Laboratory (HPCVL). NMR facilities were funded by the CFI (Project No. 19119) and the Province of Ontario. Prof. Rebecca Jockusch (University of Toronto) is gratefully acknowledged for assistance and access to instrumentation for the nanoESI-MS studies.

REFERENCES

- (1) (a) Metrangolo, P.; Meyer, F.; Pilati, T.; Resnati, G.; Terraneo, G. *Angew. Chem., Int. Ed.* **2008**, *47*, 6114–6127. (b) Beale, T. M.; Chudzinski, M. G.; Sarwar, M. G.; Taylor, M. S. *Chem. Soc. Rev.* **2013**, *42*, 1667–1680.
- (2) (a) Bleiholder, C.; Werz, D. B.; Köppel, H.; Gleiter, R. *J. Am. Chem. Soc.* **2006**, *128*, 2666–2674. (b) Bleiholder, C.; Gleiter, R.; Werz, D. B.; Köppel, H. *Inorg. Chem.* **2007**, *46*, 2249–2260. (c) Sanz, P.; Yáñez, M.; Mó, O. *J. Phys. Chem. A* **2002**, *106*, 4661–4668.
- (3) (a) Sundberg, M. R.; Ugglá, R.; Viñas, C.; Teixidor, F.; Paavola, S.; Kivekäs, R. *Inorg. Chem. Commun.* **2007**, *10*, 713–716. (b) Scheiner, S. *Cryst. Eng. Commun.* **2013**, *15*, 3119–3124.
- (4) (a) Cozzolino, A. F.; Elder, P. J. W.; Vargas-Baca, I. *Coord. Chem. Rev.* **2011**, *255*, 1426–1438. (b) Rosenfield, R. E.; Parthasarathy, R.; Dunitz, J. D. *J. Am. Chem. Soc.* **1977**, *99*, 4860–4862. (c) Row, T. N. G.; Parthasarathy, R. *J. Am. Chem. Soc.* **1981**, *103*, 477–479. (d) Cohen-Addad, C.; Lehmann, M. S.; Becker, P.; Parkanyi, L.; Kalman, A. *J. Chem. Soc., Perkin Trans. 2* **1984**, 191–196. (e) Fanfrlík, J.; Přáda, A.; Padělková, Z.; Pecina, A.; Macháček, J.; Lepšík, M.; Holub, J.; Růžička, A.; Hnyk, D.; Hobza, P. *Angew. Chem., Int. Ed.* **2014**, *53*, 10139–10142.
- (5) (a) Clark, T.; Hennemann, M.; Murray, J.; Politzer, P. *J. Mol. Model.* **2007**, *291*–296. (b) Cozzolino, A. F.; Vargas-Baca, I.; Mansour, S.; Mahmoudkhani, A. H. *J. Am. Chem. Soc.* **2005**, *127*, 3184–3190. (c) Wang, W.; Ji, B.; Zhang, Y. *J. Phys. Chem. A* **2009**, *113*, 8132–8135. (d) Tsuzuki, S.; Sato, N. *J. Phys. Chem. B* **2013**, *117*, 6849–6855. (e) Brezgunova, M. E.; Liefbrig, J.; Aubert, E.; Dahaoui, S.; Fertey, P.; Lebègue, S.; Ángyán, J. G.; Fournigué, M.; Espinosa, E. *Cryst. Growth Des.* **2013**, *13*, 3283–3289. (f) Alikhani, E.; Fuster, F.; Madebene, B.; Grabowski, S. *J. Phys. Chem. Chem. Phys.* **2014**, *16*, 2430–2442.
- (6) (a) Burling, F. T.; Goldstein, B. M. *J. Am. Chem. Soc.* **1992**, *114*, 2313–2320. (b) Nagao, Y.; Hirata, T.; Goto, S.; Sano, S.; Kakehi, A.; Iizuka, K.; Shiro, M. *J. Am. Chem. Soc.* **1998**, *120*, 3104–3110.
- (7) Fujita, K.-i.; Murata, K.; Iwaoka, M.; Tomoda, S. *Tetrahedron* **1997**, *53*, 2029–2048.
- (8) (a) Taylor, J. C.; Markham, G. D. *J. Biol. Chem.* **1999**, *274*, 32909–32914. (b) Iwaoka, M.; Takemoto, S.; Okada, M.; Tomoda, S. *Chem. Lett.* **2001**, *30*, 132–133.
- (9) Zhao, H.; Gabbai, F. *Nat. Chem.* **2010**, *2*, 984–990.
- (10) (a) Cozzolino, A. F.; Vargas-Baca, I. *J. Organomet. Chem.* **2007**, *692*, 2654–2657. (b) Berionni, G.; Pégot, B.; Marrot, J.; Goumont, R. *Cryst. Eng. Commun.* **2009**, *11*, 986–988. (c) Chivers, T.; Gao, X.; Parvez, M. *Inorg. Chem.* **1996**, *35* (1), 9–15. (d) Alcock, N. W. *Bonding and Structure: Structural Principles in Inorganic and Organic Chemistry*; Ellis Horwood, Ltd.: Harlow, U.K., 1990.
- (11) (a) Cozzolino, A. F.; Britten, J. F.; Vargas-Baca, I. *Cryst. Growth Des.* **2005**, *6*, 181–186. (b) Cozzolino, A. F.; Whitfield, P. S.; Vargas-Baca, I. *J. Am. Chem. Soc.* **2010**, *132*, 17265–17270.
- (12) Semenov, N. A.; Pushkarevsky, N. A.; Beckmann, J.; Finke, P.; Lork, E.; Mews, R.; Bagryanskaya, I. Y.; Gatilov, Y. V.; Konchenko, S. N.; Vasiliev, V. G.; Zibarev, A. V. *Eur. J. Inorg. Chem.* **2012**, *2012*, 3693–3703.
- (13) Semenov, N. A.; Lonchakov, A. V.; Kushkarevsky, N. A.; Suturina, E. A.; Korolev, V. V.; Lork, E.; Vasiliev, V. G.; Konchenko, S.

N.; Beckmann, J.; Gritsan, N. P.; Zibarev, A. V. *Organometallics* **2014**, *33*, 4302–4314.

(14) (a) Muller, C. D.; Falcou, A.; Reckefuss, N.; Rojahn, M.; Wiederhirn, V.; Rudati, P.; Frohne, H.; Nuyken, O.; Becker, H.; Meerholz, K. *Nature* **2003**, *421*, 829–833. (b) Bouffard, J.; Swager, T. M. *Macromolecules* **2008**, *41*, 5559–5562. (c) Pu, K.-Y.; Liu, B. *Macromolecules* **2008**, *41* (18), 6636–6640. (d) Grimsdale, A. C.; Leok Chan, K.; Martin, R. E.; Jokisz, P. G.; Holmes, A. B. *Chem. Rev.* **2009**, *109*, 897–1091. (e) Gibson, G. L.; Gao, D.; Jahnke, A. A.; Sun, J.; Tilley, A. J.; Seferos, D. S. *J. Mater. Chem. A* **2014**, *2*, 14468–14480. (f) Gibson, G. L.; Seferos, D. S. *Macromol. Chem. Phys.* **2014**, *215*, 811–823.

(15) Frisch, M. J. et al., *Gaussian 09*, Rev. D.01; Gaussian, Inc., Wallingford, CT, 2013.

(16) Grimme, S.; Ehrlich, S.; Goerigk, L. *J. Comput. Chem.* **2011**, *32*, 1456–1465.

(17) Weigend, F.; Ahlrichs, R. *Phys. Chem. Chem. Phys.* **2005**, *7*, 3297–3305.

(18) (a) Murray, J. S.; Lane, P.; Politzer, P. *Int. J. Quantum Chem.* **2007**, *107*, 2286–2292. (b) Politzer, P.; Murray, J. S.; Clark, T. *Phys. Chem. Chem. Phys.* **2013**, *15*, 11178–11189. (c) Kolar, M.; Hostas, J.; Hobza, P. *Phys. Chem. Chem. Phys.* **2014**, *16*, 9987–9996.

(19) (a) Sarwar, M. G.; Dragisic, B.; Salsberg, L. J.; Gouliaras, C.; Taylor, M. S. *J. Am. Chem. Soc.* **2010**, *132*, 1646–1653. (b) Dimitrijevic, E.; Kvak, O.; Taylor, M. S. *Chem. Commun.* **2010**, 46, 9025–9027. (c) Riley, K. E.; Murray, J. S.; Politzer, P.; Concha, M. C.; Hobza, P. *J. Chem. Theory Comput.* **2009**, *5*, 155–163.

(20) (a) Lommerse, J. P. M.; Stone, A. J.; Taylor, R.; Allen, F. H. *J. Am. Chem. Soc.* **1996**, *118*, 3108–3116. (b) Lu, Y.-X.; Zou, J.-W.; Wang, Y.-H.; Yu, Q.-S. *J. Mol. Struct.: THEOCHEM* **2006**, *76*, 83–87. (c) Riley, K. E.; Hobza, P. *J. Chem. Theory Comput.* **2008**, *4*, 232–242. (d) Palusiak, M. *J. Mol. Struct.: THEOCHEM* **2010**, *945*, 89–92. (e) Wolters, L. P.; Bickelhaupt, F. M. *Chem. Open* **2012**, *1*, 96–105. (f) Huber, S. M.; Jimenez-Izal, E.; Ugalde, J. M.; Infante, I. *Chem. Commun.* **2012**, 48, 7708–7710.

(21) Robertson, C. C.; Perutz, R. N.; Brammer, L.; Hunter, C. A. *Chem. Sci.* **2014**, *5*, 4179–4183.

(22) (a) Cabot, R.; Hunter, C. A. *Chem. Commun.* **2009**, 2005–2007. (b) Laurence, C.; Graton, J.; Berthelot, M.; El Ghomari, M. J. *Chem.—Eur. J.* **2011**, *17*, 10431–10444. (c) Chudzinski, M. G.; Taylor, M. S. *J. Org. Chem.* **2012**, *77*, 3483–3491.

(23) Rosokha, S. V.; Stern, C. L.; Ritzert, J. T. *Chem.—Eur. J.* **2013**, *19*, 8774–8778.

(24) Robinson, S. W.; Mustoe, C. L.; White, N. G.; Brown, A.; Thompson, A. L.; Kennepohl, P.; Beer, P. D. *J. Am. Chem. Soc.* **2015**, *137*, 499–507.

(25) Yang, R.; Tian, R.; Yan, J.; Zhang, Y.; Yang, J.; Hou, Q.; Yang, W.; Zhang, C.; Cao, Y. *Macromolecules* **2005**, *38*, 244–253.

(26) Zhou, Y.-P.; Zhang, M.; Li, Y.-H.; Guan, Q.-R.; Wang, F.; Lin, Z.-J.; Lam, C.-K.; Feng, X.-L.; Chao, H.-Y. *Inorg. Chem.* **2012**, *51*, 5099–5109.

(27) Zhao, Y.; Truhlar, D. *Theor. Chem. Acc.* **2008**, *120*, 215–241.

(28) Bauzá, A.; Alkorta, I.; Frontera, A.; Elguero, J. *J. Chem. Theory Comput.* **2013**, *9*, 5201–5210.

(29) Another set of calculations was carried out, using Grimme's dispersion correction to the M06-2X functional (M06-2X-D3). A slight improvement in terms of agreement between calculated and experimental free energies of interaction was observed over M06-2X, but this did not significantly change the relative performance of the B97 and M06-2X functionals. See the Supporting Information for details.